Colloids and Surfaces A: Physicochemical and Engineering Aspects 666 (2023) 131287

Contents lists available at ScienceDirect

Colloids and Surfaces A: Physicochemical and Engineering Aspects

journal homepage: www.elsevier.com/locate/colsurfa

Development of colloidal lignin particles through particle design strategies and screening of their Pickering stabilizing potential

Giovana Colucci [a,b,c,d], Arantzazu Santamaria-Echart [a,b], Samara C. Silva [a,b,c,d], Liandra G. Teixeira [a,b,c,d], Andreia Ribeiro [c,d], Alírio E. Rodrigues [c,d], M. Filomena Barreiro [a,b,*]

[a] Centro de Investigação de Montanha (CIMO), Instituto Politécnico de Bragança, Campus de Santa Apolónia, 5300–253 Bragança, Portugal
[b] Laboratório Associado para a Sustentabilidade e Tecnologia em Regiões de Montanha (SusTEC), Instituto Politécnico de Bragança, Campus de Santa Apolónia, 5300–253 Bragança, Portugal
[c] Laboratory of Separation and Reaction Engineering (LSRE-LCM), Faculdade de Engenharia, Universidade do Porto, R. Dr. Roberto Frias, S/N, 4200–465 Porto, Portugal
[d] Associate Laboratory in Chemical Engineering (ALiCE), Faculdade de Engenharia, Universidade do Porto, R. Dr. Roberto Frias, S/N, 4200–465 Porto, Portugal

GRAPHICAL ABSTRACT

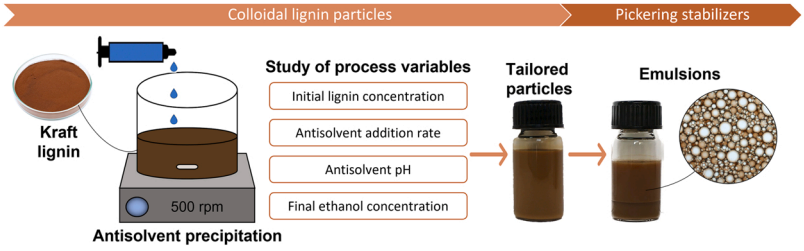

ARTICLE INFO

Keywords:
Lignin
Colloidal Particles
Screening Design
Process Variables Effects
Pickering Stabilizers

ABSTRACT

Colloidal lignin particles (CLPs) have increased interest as green and sustainable materials for Pickering stabilizers, with particle design being an important step towards their effective use. In this context, the antisolvent precipitation method was selected to conduct a study aiming at understanding the effect of process variables (initial lignin concentration, antisolvent pH, final ethanol concentration, and antisolvent addition rate) on particle size, zeta potential, color parameters, and contact angle. Moreover, their Pickering stabilizing potential was preliminarily screened. The evaluation using a Fractional Factorial Design revealed that the particle size is significantly influenced by the initial lignin concentration (as it increases, larger particles are obtained) and the final ethanol concentration (as it increases, smaller sizes result). The zeta potential is significantly affected by the antisolvent pH and the initial lignin concentration; the increase in both parameters results in higher negative values. The color is significantly dependent on the used initial lignin concentration (as it increases, particles become lighter and the yellowish accentuates) and the antisolvent pH (as it increases, particles become darker). Both initial lignin concentration and final ethanol concentration increase promote hydrophobicity, whereas increasing the antisolvent pH and its addition rate turns particles more hydrophilic. Through this strategy, it was

* Corresponding author at: Centro de Investigação de Montanha (CIMO), Instituto Politécnico de Bragança, Campus de Santa Apolónia, 5300–253 Bragança, Portugal.
E-mail address: barreiro@ipb.pt (M.F. Barreiro).

https://doi.org/10.1016/j.colsurfa.2023.131287
Received 28 November 2022; Received in revised form 9 March 2023; Accepted 12 March 2023
Available online 17 March 2023

possible to achieve CLPs with promising Pickering stabilizing potential, putting in evidence the importance of understanding the production process to design effective particles for target applications.

1. Introduction

Lignin, the most abundant aromatic biopolymer in nature, has attracted increased attention over the years due to its potential as a renewable raw material to produce aromatic compounds and materials [1,2]. It is mainly available as technical lignins derived from the by-products of the paper/pulp and bioethanol industries, being produced in amounts reaching millions of tons per year [3]. Despite this high potential, more than 95 % of the black liquor in the pulp and paper industry is still burned to recover energy. Searching for new high-value-added alternatives is essential for establishing biorefineries and adopting a circular bioeconomy [2,4]. Lignin contributes to carbon fixation in materials, minimizing global warming and being an alternative to fossil-based compounds [5,6].

The potential of lignin has been proven in a wide range of applications, including biofuels, binders, dispersants, polymeric materials, and packaging [7,8]. However, its use as a raw material can face limitations due to its highly complex and random structure and low water solubility [8]. In this context, colloidal lignin particles (CLPs) production has been addressed as a promising strategy since they can turn lignin water-dispersible without any chemical modification. Moreover, the particles' high surface area-to-volume and shape positively affect lignin properties, increasing antioxidant and UV protection, antimicrobial activity, and thermal stability [6,9,10].

Among the numerous applications of CLPs, their use as Pickering stabilizers has gained interest due to their ability to be adsorbed at the oil-water interfaces promoting emulsion stabilization [11]. Lignin-based Pickering stabilizers are a potential alternative to conventional synthetic surfactants due to their biodegradability and renewability. Besides that, this new focus expands lignin's applications to areas such as cosmetics, pharmaceuticals, and food [6,12]. For example, Bertolo et al. [13] prepared kraft and organosolv lignin particles to be used as Pickering stabilizers to produce curcumin-loaded emulsions, potentiating the pharmacological attributes of this polyphenol, and Cuthill et al. [14] extracted lignin from cocoa shells to prepare colloidal lignin-rich particles, which were applied as Pickering stabilizers in emulsions for food applications.

Using lignin particles as Pickering stabilizers implies the need to control the CLPs production process. Among the various available techniques, antisolvent precipitation is the most used method due to its simplicity, low cost (dependent on the used solvent), ability to control the particle size and morphology, and ability to achieve high particle yields [5,15]. The method comprises lignin solubilization in an aqueous organic solvent, followed by adding water as an antisolvent to decrease solubility. This step promotes lignin precipitation and self-assembling into small particles to minimize the surface area in contact with the antisolvent [4–6]. The selection of the organic solvent must consider aspects such as cost, toxicity, environmental impact, and other hazards, which may result in limitations for CLPs industrial scale-up and use in bio-applications. In this context, most published works had applied toxic solvents such as tetrahydrofuran [16–18], methanol [19,20], and dimethyl sulfoxide [13,21]. The use of ethanol, considered a green, biocompatible, and cost-effective solvent, started to be reported more recently [2,8,22,23].

To optimize CLPs production, the impact of the process variables on the particles' properties must be identified and understood [6]. For example, it has been reported that the initial lignin concentration influences the particle size and stability, with particles starting to aggregate and sediment after a specific concentration [2,7,24]. For this reason, most studies do not surpass the use of 10 g/L [14,22]. Furthermore, the final solvent concentration, i.e., the solvent concentration after the antisolvent diluting step, is also a relevant parameter influencing particle formation, size, and stability [2,6,25]. Leskinen et al. [25], in a work producing CLPs from a kraft lignin by nanoprecipitation from THF-water systems, observed that stable particles were only formed when the final THF concentration was within 25 %– 20 % (v/v). It was also reported that the antisolvent addition rate impacts the particle size [25]. The antisolvent pH can also be a relevant variable, influencing particle formation and stabilization mechanisms due to its effect on lignin electrostatic interactions [25–27]. However, this parameter is often neglected and rarely addressed in the published literature, as pointed out by Österberg et al. [6] in a recent literature review.

In this context, this work aimed to perform a screening design using a Fractional Factorial Design (FFD) to understand the individual effect of process variables on CLPs' properties, including their potential to act as Pickering stabilizers and identify the most significant ones. For this, the antisolvent precipitation method was applied with a commercial kraft lignin, Indulin AT, and ethanol, a green and recyclable solvent alternative. The process variables were the initial lignin concentration, the antisolvent pH, the final ethanol concentration, and the antisolvent addition rate. As CLPs' properties (FFD responses), the particle size, zeta potential, contact angle, and color (important sensorial attribute, e.g., for cosmetic applications) were selected. Moreover, the CLPs' ability to act as Pickering stabilizers was accessed. Even though studies addressing the evaluation of process variables can be found in the literature, to the authors' best knowledge, this is the first one where a systematization of their effects was performed. This strategy presents several advantages, helping to design and prepare tailored CLPs for target applications, e.g., Pickering stabilizers, an emerging field of cosmetic and food applications.

2. Materials and methods

2.1. Materials

Indulin AT, kindly supplied by Ingevity™, is a purified form of kraft pine lignin (purity 97 %). Citrate phosphate buffer solutions with a molarity of 0.1 mol/L were prepared using di-sodium hydrogen phosphate anhydrous (Panreac, Spain) and citric acid (Merck, Germany). Sodium hydroxide (NaOH) and hydrochloric acid (HCl, 37 %) were purchased from Sigma-Aldrich (Germany). Ethanol absolute (purity $\geq$ 99.8 %) was purchased from Riedel-de Haën (Germany). Miglyol 812 was purchased from Acofarma (Spain). The used water was distilled water.

2.2. Screening design for CLPs production

Screening design is a robust statistical tool used to analyze the individual effect and statistical significance of process variables on target responses, using a reduced number of experiments [28]. A Fractional Factorial Design (FFD) including 2^{4-1} assays plus three central points (total of 11 experimental runs) was applied to evaluate the effect of four independent variables (initial lignin concentration (x_1, g/L), antisolvent pH (x_2), final ethanol concentration (x_3, v/v), and antisolvent addition rate (x_4, mL/min), on selected responses (particle size (nm), zeta potential (mV), color (expressed using CIELAB space), and contact angle (°)).

The initial lignin concentration was set from 10 to 50 g/L to consider the production of concentrated particle dispersions. Most reported studies are limited to 10 g/L, being this parameter an essential point from an industrial perspective. The antisolvent pH was set from 4 to 8, guaranteeing an extensive range to inspect the effect of this variable. The antisolvent addition rate was established from 6 to 14 mL/min (corresponding to a dilution rate from 0.15 to 0.35 min^{-1}; Dilution rate=Addition rate/Initial volume). Although faster addition rates have been applied in other studies [2,25], the selected range was considered suitable for the used experimental scale (initial volume of lignin solution = 40 mL). Under these conditions, the antisolvent (volume from 22 to 147 mL), is added between 1 and 25 min. The same production time can be reached for higher scales by determining the antisolvent addition rate needed for the same dilution rate. The final ethanol concentration was defined from 15 % to 45 % (v/v), based on other reported works supporting the successful formation of particles in this range [2,25].

The coded levels (real values in parentheses) for the defined 11 experimental runs are presented in Table 1. The reproducibility of the process was checked by doing 3 replicates at the central point (Runs 9, 10, and 11). From the FFD 2^{4-1}, the statistically significant variables at a 10 % significance level (p-value $\leq$ 0.10) were identified, and the effects were generated by TIBCO Statistica 12 software (Statsoft Inc, USA). The defined experimental runs were executed randomly.

2.3. CLPs preparation procedure

The CLPs were produced based on the experimental procedure reported by Sipponen et al. [2] with some modifications. Firstly, a solubility screening using the highest studied concentration (50 g/L) was performed to define the most appropriate ethanol/water ratio to solubilize the lignin. For the ethanol/water ratio of 70/30 (v/v), a soluble fraction of 92 % (46 g/L) was achieved, guarantying complete solubilization for lower concentrations. Considering the nature of the antisolvent (buffer solutions with the presence of salts), its addition can further facilitate lignin solubilization, and thus the 50 g/L samples were also considered in the study. Then, lignin solutions (40 mL) were prepared under stirring for 10 min (500 rpm, magnetic stirrer) at the desired initial lignin concentration. The antisolvent (an aqueous phosphate-citrate buffer solution with the needed pH) was added to the lignin solution at a controlled addition rate using a syringe pump (KDS 200, KD Scientific, USA). The amount of the added antisolvent was varied to reach the planned final ethanol concentration. Finally, the ethanol was removed and the resultant CLPs dispersions were concentrated up to the initial volume (40 mL) in a rotary evaporator (Büchi R-11, Büchi, Switzerland) at 60 °C and 180–140 mbar, then stored at room temperature protected from light. By doing this step the final lignin concentration will be the same as the initial lignin concentration. The complete conditions used to prepare the CLPs are reported in Table 1.

Table 1
Coded levels (real values in parentheses) for the experimental design (initial lignin concentration (x_1, g/L), antisolvent pH (x_2), final ethanol concentration (x_3, % v/v), and antisolvent addition rate (x4, mL/min)).

	Process variables			
Run	x_1	x_2	x_3	x_4
1	-1 (10)	-1 (4)	-1 (15)	-1 (6)
2	+1 (50)	-1 (4)	-1 (15)	+1 (14)
3	-1 (10)	+1 (8)	-1 (15)	+1 (14)
4	+1 (50)	+1 (8)	-1 (15)	-1 (6)
5	-1 (10)	-1 (4)	+1 (45)	+1 (14)
6	+1 (50)	-1 (4)	+1 (45)	-1 (6)
7	-1 (10)	+1 (8)	+1 (45)	-1 (6)
8	+1 (50)	+1 (8)	+1 (45)	+1 (14)
9	0 (30)	0 (6)	0 (30)	0 (10)
10	0 (30)	0 (6)	0 (30)	0 (10)
11	0 (30)	0 (6)	0 (30)	0 (10)

2.4. CLPs particle size determination

The particle size of the CLPs was measured by laser diffraction using a Mastersizer 3000 equipped with a Hydro MV dispersion unit (Malvern Instruments Ltd., United Kingdom). The refractive index and absorption of the particles were set to 1.6 and 0.1, respectively, following published data [24,29]. CLPs were added as such in the dispersing media (distilled water) until achieving an obscuration of about 3.5 %, at a rotation of 2000 rpm, and at room temperature. Five consecutive measurements were done for each sample. The results were expressed as number-size distributions, and the median particle diameter (D50) was used for size analysis. The results are reported as average ± standard deviation (SD).

2.5. CLPs zeta potential determination

The zeta potential of the CLPs was determined by particle electrophoresis using a Nano-ZS Zetasizer instrument (Malvern Instruments Ltd., United Kingdom) equipped with a standard DTS1070 disposable folded capillary cell. For the assays, the samples were diluted in distilled water at 2.5 g/L. All measurements were carried out in triplicate at room temperature using values of 1.6 and 0.1 for the refractive index and absorption, respectively. The results are reported as average ± SD.

2.6. CLPs color attributes

The color of the CLPs was measured using a colorimeter CR-400 (Konica Minolta, Japan), where the L*, a*, and b*(CIELAB space) color parameters were determined. CLPs dispersions were gently stirred to obtain a representative homogeneous suspension sample for the color measurements. The measurements were performed in triplicate, and the results are reported as average ± SD.

2.7. Contact angle measurements

The water-in-air contact angle of the CLPs, taken as an indicator of their hydrophilic character, was determined using an optical contact angle device (Theta Lite 100, Biolin Scientific, Sweden). For the analysis, CLPs were dried in an oven at 70 ºC for at least 24 h, and pristine lignin was used as such. Then, pellets with a diameter of 13 mm and a thickness of about 1 mm were prepared using a hydraulic press (Specac Ltd., United Kingdom) at 10 tonnes for 2 min. The pellets' surface was previously checked by optical microscopy (Nikon Eclipse 50i, Nikon Corporation, Japan) to discard the ones with surface cracks. Measurements were made by pouring a sessile drop of distilled water (10 μL) at the pellet surface using a high-precision injector. The droplet was recorded for 60 s with a high-speed video camera coupled to the equipment. The contact angle values between the droplet and the pellet surface (left and right) were automatically calculated by the software One Attens using the Laplace-Young equation. Measurements were performed in triplicate using independent pellets. The results are reported as average contact angles from 10 to 50 s, and the images were taken 30 s after water drops at the surface.

2.8. CLPs Pickering stabilizing potential

The ability of the CLPs to act as Pickering stabilizers was determined based on the measurement of the formed emulsified layer (EL, Eq. 1). For that, subsequently to particle production, equal volumes of an aqueous phase (aqueous dispersion of CLPs used as such) and an oil phase (Miglyol 812) were mixed and vortexed for 60 s. The resulting emulsions were stored at room temperature and protected from light. The emulsions were photographically registered and analyzed by optical microscopy using a Nikon Eclipse 50i (Nikon Corporation, Japan) equipped

with Nikon Digital and NIS-Elements Documentation software. EL was determined after 1 and 30 days of storage. The results for 1 day were used to evaluate the Pickering stabilizing potential, and the results for 1 month were used to have the first insights concerning stability issues.

$$EL\% = H_E \times 100/H_T \quad (1)$$

where H_E is the height of the emulsified layer, and H_T is the total sample height.

2.9. Transmission electron microscopy (TEM)

TEM analysis was performed using a JEOL JEM 1400 TEM 120 kV apparatus (Japan). For this, CLPs were diluted at a 1:40 ratio with distilled water, and 10 μL of the sample was dropped on Formvar/carbon film-coated mesh nickel grids (Electron Microscopy Sciences, USA), then left to stand for 2 min. The liquid in excess was removed with filter paper. Images were digitally recorded using a CCD digital camera Orious 1100 W.

3. Results and discussion

3.1. Analysis of the CLPs production

The CLPs were prepared by the antisolvent precipitation method using a mixture of ethanol/water 70/30 (v/v) as the solvent. The main objective was to design suitable particles to act as Pickering stabilizers. For that, understanding the effect of process variables on key particles' properties is essential. Moreover, it is also critical to render the process more attractive at the industrial level achieving the use of high initial lignin concentration, which impacts the mass of formed CLPs. All the achieved characterizations for the performed FFD 2^{4-1} runs (11 in total) (particle size, zeta potential, contact angle, and color parameters (L*, a*, and b*)) can be found in Table S1 of the Supplementary material.

Table 2 lists the estimated individual effects of each process variable (initial lignin concentration, antisolvent pH, final ethanol concentration, and antisolvent addition rate) on the defined responses. Within the analyzed variable ranges, when the effect has a positive value (+) it indicates that an increase in the variable causes an increase in the analyzed response. If the value is negative (-), the variable increase produces a decrease in the analyzed response. The standard error (Std. Err.) gives an estimation of the samples' variability. It is used to calculate the t-value using a t-test hypothesis with 5 degrees of freedom, labeled as t(5). The p-value indicates the significance probability of the t-test. In this screening design, a significance level of 10 % (p-value $\leq$ 0.10) was chosen, which means that if a variable's effect presents a p-value lower than or equal to 0.10, then it is statistically significant in the analyzed response [28].

3.1.1. Effect of process variables on particle size

The particle size is reported to affect the stability of Pickering emulsions. Particles with too large sizes may not be able to completely cover the oil droplets, resulting in unstable emulsions [30,31]. On the other hand, particles with too small sizes (lower than 100 nm) are not appropriate due to regulatory issues in biological applications, such as cosmetics [32]. Fig. 1a presents the determined particle size for each run defined according to the FFD 2^{4-1} design matrix. Particle size distributions and span can be consulted in the Supplementary material (Fig. S1). Most samples, except CLPs 4 and 7, presented particle sizes from 200 to 500 nm, which is a suitable size range to prepare Pickering emulsions, as reported by Li et al. [30].

The effect of the antisolvent precipitation process variables (initial lignin concentration, antisolvent pH, final ethanol concentration, and antisolvent addition rate) on the particle size is reported in Table 2. Although presenting a p-value equal to 0.1205, the effect of the initial lignin concentration on the particle size was considered significant due to the proximity with the used significant level (p-value $\leq$ 0.10). This is an important consideration for further optimization studies, to prevent a relevant process variable from being erroneously discarded. Moreover, this consideration does not affect the effect analysis [28]. The initial lignin concentration positively affected the particle size, namely when it changed from 10 to 50 g/L, an increase of 196 nm resulted in the particle size. Sipponen et al. [2], in their study of CLPs production using wheat straw soda lignin solubilized in ethanol 7/3 (v/v) (87 % soluble fraction), observed a molecular weight-dependent precipitation pattern, from high to low molecular weight (Mw). Since high Mw lignin fragments are less soluble, they precipitate first, forming the particle nuclei. The particle growth occurs as other lignin fragments precipitate and

Table 2
Effect of the process variables initial lignin concentration (x_1, g/L), antisolvent pH (x_2), final ethanol concentration (x_3, % v/v), and antisolvent addition rate (x4, mL/min) in the FFD 2^{4-1} for the studied responses (particle size (nm), zeta potential (mV), color parameters (L*, a* and b*), and contact angle (°)).

Factor	Particle size				Zeta potential				Contact angle			
	Effect (nm)	Std. Err.	t (5)	p-value	Effect (mV)	Std. Err.	t (5)	p-value	Effect (°)	Std. Err.	t (5)	p-value
Mean	398.99	52.42	7.61	0.0006[a]	-26.46	1.22	-21.73	0.0000[a]	29.89	3.07	9.74	0.0002[a]
Curvature	-234.64	200.75	-1.17	0.2952	-21.54	4.66	-4.62	0.0057[a]	14.14	11.75	1.20	0.2829
x_1	196.03	104.84	1.87	0.1205[b]	-9.10	2.43	-3.74	0.0135[a]	6.40	6.14	1.04	0.3449
x_2	-54.53	104.84	-0.52	0.6252	-18.27	2.43	-7.50	0.0007[a]	-7.30	6.14	-1.19	0.2877
x_3	-244.03	104.84	-2.33	0.0674[a]	-3.91	2.43	-1.61	0.1689	7.69	6.14	1.25	0.2655
x_4	-115.48	104.84	-1.10	0.3209	1.26	2.43	0.52	0.6259	-2.32	6.14	-0.38	0.7214

Factor	Color parameters											
	L*				a*				b*			
	Effect	Std. Err.	t(5)	p-value	Effect	Std. Err.	t(5)	p-value	Effect	Std. Err.	t(5)	p-value
Mean	38.97	1.44	27.11	0.0000[a]	6.62	0.36	18.36	0.0000[a]	12.08	1.35	8.95	0.0003[a]
Curvature	9.17	5.51	1.67	0.1565	1.21	1.38	0.88	0.4195	5.63	5.17	1.09	0.3254
x_1	6.98	2.87	2.43	0.0595[a]	0.83	0.72	1.14	0.3046	5.87	2.70	2.18	0.0815[a]
x_2	-10.93	2.87	-3.80	0.0126[a]	-3.63	0.72	-5.04	0.0040[a]	-12.41	2.70	-4.60	0.0058[a]
x_3	1.48	2.87	0.51	0.6294	-0.23	0.72	-0.32	0.7594	1.29	2.70	0.48	0.6517
x_4	1.50	2.87	0.52	0.6245	0.77	0.72	1.07	0.3346	2.55	2.70	0.95	0.3879

[a] Significant factor (p-value $\leq$ 0.10)
[b] Considering the proximity of 0.1205 with the established significance level, the initial lignin concentration was considered a significant factor for the particle size response.

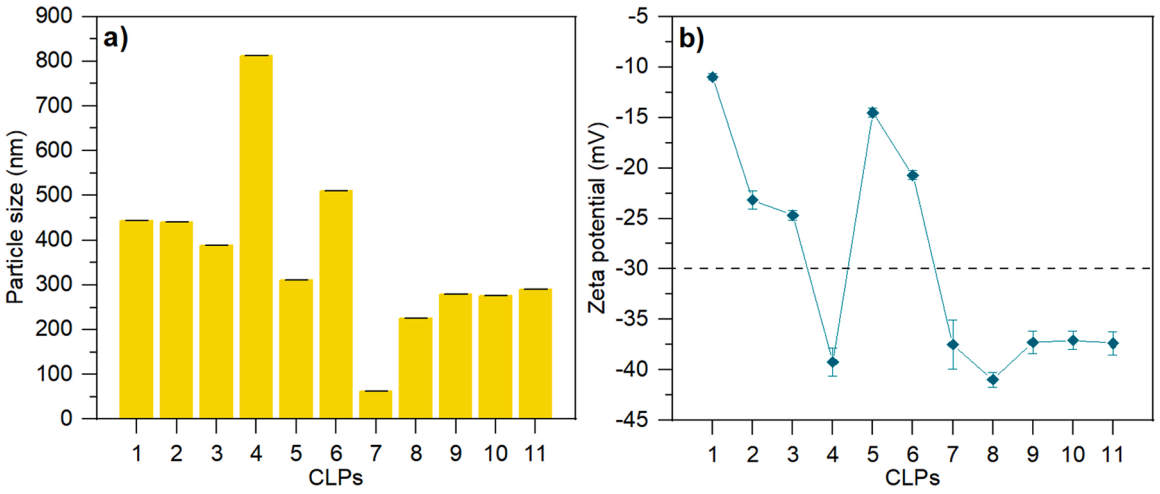

Fig. 1. CLPs properties for the 11 runs: (a) particle size and (b) zeta potential. The dashed line separates the zeta potential stable region (below) from the unstable region (above).

assemble into the existing particles. Particle formation ends with two parallel events: the surface orientation of the hydrophilic segments and the adsorption of small polar lignin fragments. Similarly to this work, the authors reported a particle size increase with initial lignin concentration increase; i.e., higher initial lignin concentration increases lignin availability to participate in the nucleation-growth process, resulting in larger particles. This behavior was also reported in other studies that produced CLPs from different solvent systems [24,33,34].

The final ethanol concentration presented a negative significant effect on the particle size (p-value = 0.0674), meaning that the higher the final ethanol concentration is (45 %), the smaller CLPs are obtained. This result agrees with the work of Sipponen et al. [2] dealing with the study of the controlled nucleation-growth mechanism of CLPs from aqueous ethanol systems. It was observed that small nuclei particles are formed at the starting point (higher ethanol concentration) and that the antisolvent addition (decrease of ethanol concentration), intensifies its lignin precipitation and association with the formed small nuclei, generating larger particles [2].

Previous studies have reported that the antisolvent addition rate influences particle size, namely its increase resulting in particle size reduction [2,25,35]. Even though this behavior was also observed in this work (a negative effect of the antisolvent addition rate on the particle size was observed), the effect was not significant (p-value = 0.3209). This indicates that, for the studied range (6–14 mL/min), any value can be selected without impacting particle size. The antisolvent pH was also a non-significant variable for the particle size (p-value = 0.6252).

3.1.2. *Effect of process variables on zeta potential*

Lignin is a negatively charged polymer due to the presence of phenols, carboxylic acids, and hydroxyl ions [36]. As expected, all the particles presented negative zeta potential values, namely between − 10.96 and − 40.98 mV (Fig. 1b). Values higher than + 30 mV or lower than − 30 mV indicate that the particles have a sufficient electrical double layer hindering aggregation, indicating colloidal stability [8]. In this study, only CLPs 4, 7, 8, and the central points (CLPs 9–11) presented zeta potential values in the stable range.

The most significant variable influencing zeta potential was the antisolvent pH (p-value = 0.0007). Increasing the antisolvent pH from 4 to 8 decreased the zeta potential at about 18 mV, meaning that the CLPs became more stable. This observation agrees with studies reporting that the negative surface charge driving CLPs stability is related to the carboxylic acid groups in lignin's structure [25]. Increasing the pH intensifies lignin's carboxylic acids deprotonation, thus the CLPs' negative surface charge, leading to electrostatic stabilization [6,37]. Using an antisolvent pH of 6 or 8 (higher than the pKa value of lignin's carboxyl groups (5.5) [38]) increased the negative charge of the CLPs and thus their stability. No deprotonation of phenolic and aliphatic hydroxyl groups is expected in the studied pH range. Leskinen et al. [25], who studied the effect of using alkaline solutions (NaOH) as the antisolvent, found that CLPs stabilization was improved, particularly for samples using high initial lignin concentration (4 wt%). These results are in accordance with the ones of the present work, considering that CLPs prepared using an initial lignin concentration of 50 g/L were stable at pH 8 (CLPs 4 and 8) but unstable at pH 4 (CLPs 2 and 6).

The initial lignin concentration had a significant negative effect on zeta potential (p-value = 0.0135). This means that under the studied conditions, the zeta potential decreases as the initial lignin concentration increases, resulting in improved CLPs' dispersion stability. Similar behavior was observed by Zhang et al. [39] on CLPs prepared by the antisolvent precipitation method using a deep eutectic solvent. A decrease in the zeta potential from − 5 mV to − 26 mV was observed when the initial lignin concentration went from 0.5 to 5 g/L. The obtained trend was justified due to the variable lignin availability during the self-assembly process, which causes different thermodynamic equilibrium states [39]. In fact, the obtained behavior is complex and requires further investigation. One hypothesis is that it is related to the particle size obtained at different initial lignin concentrations. In this

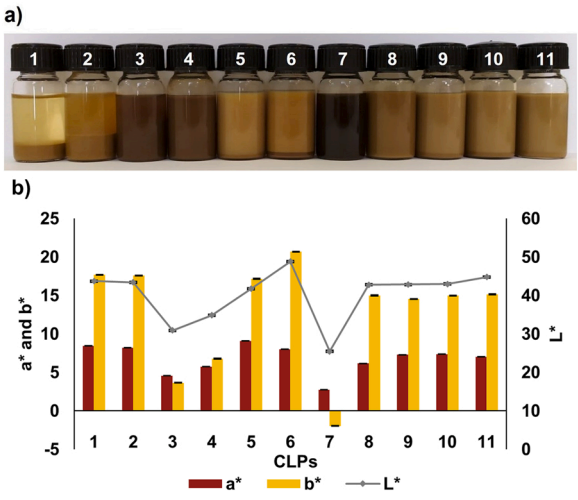

Fig. 2. (a) Images of CLPs taken with a digital camera. (b) L*, a*, and b* parameters from the CIELAB color space for each CLPs.

sense, bigger particles may have a higher density of charged groups on their surfaces, resulting in higher zeta potentials (in absolute values). Regarding the other variables, namely, the final ethanol concentration and the antisolvent addition rate, they did not significantly affect the zeta potential.

3.1.3. Effect of process variables on color attributes

Color plays a vital role in commercial applications, e.g., coatings, packaging, and cosmetics [3,23]. The visual appearance of the CLPs dispersions is shown in Fig. 2a, putting in evidence the obtained range of tones. The color hue was characterized using the CIELAB-color space and expressed according to three parameters: L*, a*, and b*. L* indicates the luminosity (0 (dark) to 100 (light)), a* the red-green component that goes from green (−60) to red (60), and b* the blue-yellow component (blue (−60) to yellow (60)) (Fig. 2b). The darker samples (CLPs 3, 4, and 7) presented the lowest L* values (25−35) and similar absolute a* and b* values. In contrast, the other samples exhibited L* values in the range of 40–50 and b* values higher than a* values, evidencing their yellowish hue.

Kraft lignins usually present a dark brown color due to the harsh conditions used in the extraction process; being important to control these attributes for high-value-added products. Transforming pristine lignin into colloidal particles has been reported to result in lighter products [40]. The present study shows that CLPs color is highly dependent on the production conditions, namely lighter (L* increase) and more yellowish (b* increase) samples are obtained when the initial lignin concentration increases. In contrast, darker brown samples are obtained as the antisolvent pH changes from 4 to 8. According to the particle formation self-assembly mechanism, a rise in the initial lignin concentration contributes to increasing the number of formed particles (higher particle yield), which may justify the reason why samples produced from higher lignin concentrations are lighter. On the other hand, pH increase promotes lignin solubility, and thus the formation of a lower number of particles (lower particle yield), resulting in darker colors as some lignin remains in the solution.

3.1.4. Effect of process variables on CLPs wettability

Wettability is an important parameter for Pickering stabilizers since it is a measure of the degree of hydrophilicity/hydrophobicity. Particles must present intermediate hydrophilicity to attach to the oil-water interface [30]. Particles that are too hydrophilic or hydrophobic will remain in solution (water or oil, respectively) being not adsorbed at the oil-water interface [41].

The hydrophilic character of CLPs was accessed by measuring the water-in-air contact angle. Fig. 3 shows the contact angle images for the pristine lignin Indulin AT and respective CLPs. All the samples presented contact angles lower than 90º, compatible with a hydrophilic nature [13]. Moreover, CLPs showed contact angles lower than those obtained for the pristine Indulin AT, evidencing a more pronounced hydrophilic character for the CLPs. This behavior can be associated with the lignin self-assembling process during CLPs' formation. The antisolvent precipitation method modifies the lignin hydrophilicity as the hydrophobic groups of the self-assembled lignin remain in the particle core. In contrast, the hydrophilic ones turn towards the particle surface, making the CLPs water dispersible [5].

Bertolo et al. [13] have compared the contact angles of CLPs prepared using two lignin types (alkali and organosolv) and two production techniques (solvent shifting and dialysis). They found that both the lignin type and the production method influenced the contact angle, with the solvent shifting technique generating CLPs with higher hydrophilicity (contact angles of 17.0º and 23.1º, for alkali and organosolv, respectively) compared with the dialysis process (contact angles of 31.0º and 56.0º, for alkali and organosolv, respectively) with the alkali lignin being more hydrophilic than the organosolv. In the present work (Fig. 3), by varying the process variables of the antisolvent precipitation technique, particles within an extensive range of contact angles (from 9º to 41º) were obtained, which were also more hydrophilic than the pristine lignin Indulin AT (48º).

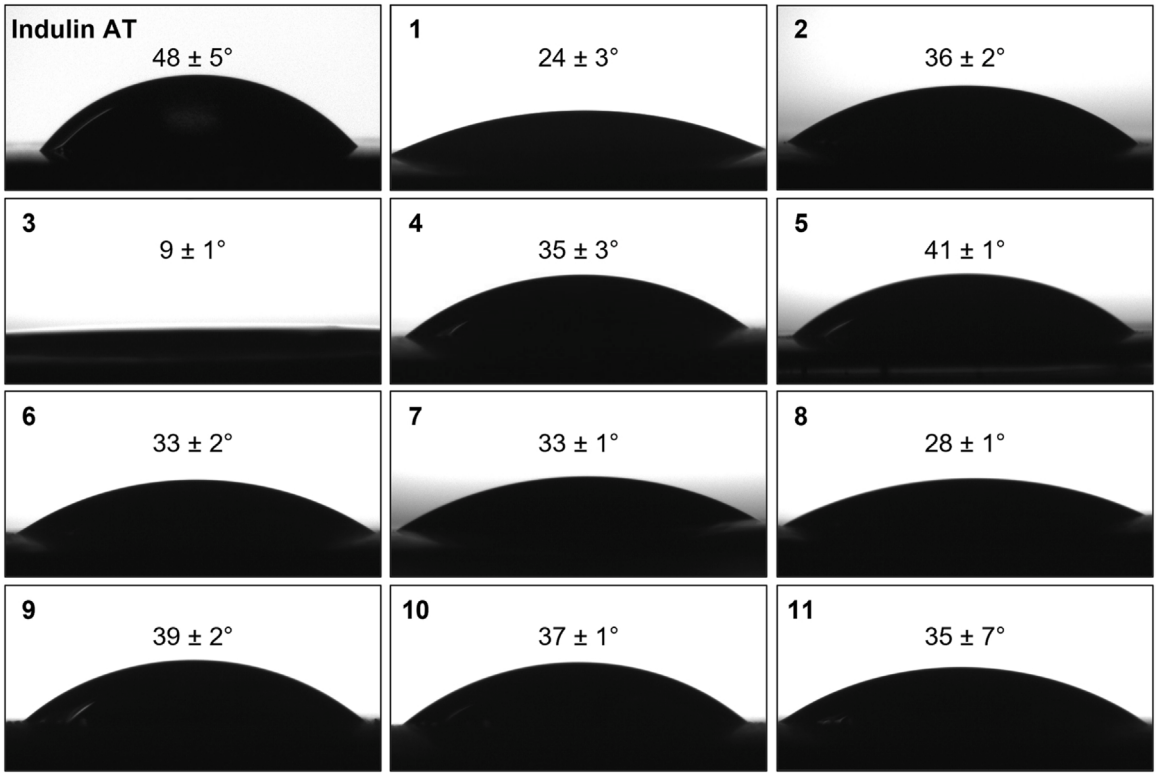

Fig. 3. Water-in-air contact angles for lignin Indulin AT and CLPs samples. Images were taken 30 s after water drops at the surface and contact angle values are the average contact angles from 10 to 50 s.

Regarding the lignin type, its heterogenous nature influences the hydrophilic characteristics. For example, a contact angle of 57 ° was reported for Indulin AT, a softwood kraft lignin, whereas for an organosolv lignin a more hydrophobic character was identified (contact angle of 69º) [11]. In the present work, a contact angle of 48º was achieved for Indulin AT. This discrepancy can be justified by the used sample preparation procedure (spin-coated lignin films against lignin pellets in this work) and the measurement time (10 s against the use of an average from 10 s to 50 s in this work). Nevertheless, the observed trends of the two works agree.

Considering the analysis of the effects, the initial lignin concentration and the final ethanol concentration increase raises the contact angle and thus the hydrophobicity. On contrary, the increase of the antisolvent pH and of the antisolvent addition rate turns particles more hydrophilic. Even though, within the studied ranges, none of the studied process variables had a significant impact on the CLPs contact angle (p-values > 0.10). Furthermore, although a microscopic inspection was made on the pellets' surface to minimize the variability of the used samples, the surface roughness at the micro/nanoscale was not measured, which may also have influenced the obtained contact angle values.

3.2. Evaluation of the Pickering stabilizing potential

Considering the rising interest in the development of biological particles to be used in the production of Pickering emulsions, the Pickering stabilizing potential of the 11 produced CLPs was tested by measuring the magnitude of the formed emulsified layer. For this, the produced CLPs suspension (water phase) and Miglyol 812 (oil phase) were mixed using a 50:50 vol ratio. The formed emulsified layer was evaluated after one day (to check the Pickering stabilizing potential) and one month (to preliminary access stability issues).

Fig. 4a shows the visual aspect of the obtained samples, taken one day after production, evidencing the formed emulsified layer together with the corresponding calculated values. Fig. 4b shows the microscopic images of a sample taken from the emulsified layer. For the samples prepared with CLPs 1, 2, and 7, which did not form emulsions, aliquots were taken in the region close to the oil/water interface, where some degree of phase mixture was observed. For the analyzed samples, the optical microscopy revealed the typical round shape of the droplets with no signs of coalescence. Moreover, due to CLPs' hydrophilic character, as previously depicted from the measured contact angles, they were expected to form oil-in-water emulsions. This was confirmed by the drop test (data not shown), in which the emulsion drops were miscible in water but immiscible in oil.

Although the particles' degree of hydrophilicity/hydrophobicity plays an important role in Pickering stabilization, other factors such as particle concentration and size are reported to impact emulsion formation and stability [11,13]. A higher particle concentration promotes better droplet coverage, and particles with larger sizes require higher energy to be removed from the oil/water interface [11]. For example,

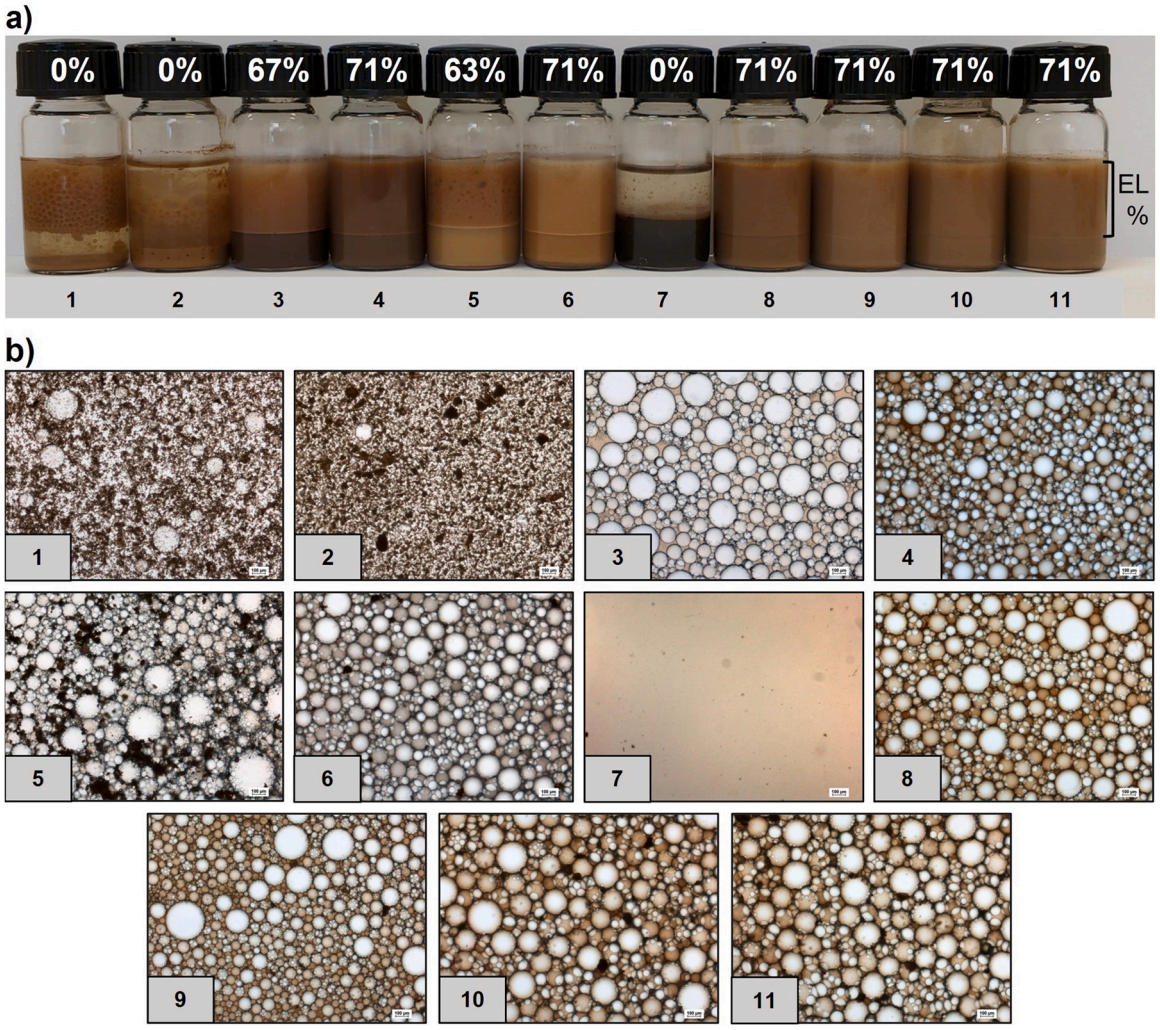

Fig. 4. (a) Images of the fresh emulsions prepared with CLPs with the percentage of emulsified layer (EL%) formed after one day of storage. (b) Optical microscopy of the emulsions (emulsified layer). The bars in the bottom right corner indicate 100 μm - magnification of 40×.

CLPs 7, although presenting intermediate hydrophilicity (33º), correspond to the lowest lignin concentration (10 g/L) and the lowest particle size (61.9 nm), and, thus, were not able to act as Pickering stabilizers. On the other hand, CLPs produced with higher lignin concentrations and holding higher particle sizes, such as CLPs 4, 6, and 8, could form stable emulsified layers.

The stability of CLPs, evaluated through the zeta potential, also affects Pickering emulsion formation. In this view, although CLPs 1 and 2 presented positive characteristics to form emulsions, such as intermediate hydrophilicity and suitable particle size (443 and 441 nm, respectively), both particles had zeta potentials higher than − 30 mV (Fig. 1b). They presented signs of precipitation, as can be inspected in Fig. 2a. Furthermore, CLPs 3 and CLPs 5 also produced emulsion samples with apparent instability (mainly after the storage period of 30 days, Fig. 5a), which may be related to their low zeta potential absolute values. This result highlights the importance of preparing CLPs able to form stable water dispersions, an intermediate step for Pickering emulsions preparation.

Fig. 5a shows the visual aspect of the obtained samples, together with the calculated emulsified layer percentage, taken one month after the production. Fig. 5b shows the corresponding microscopic images to check for instability phenomena development (e.g., droplet coalescence). Compared with Fig. 4a and b, it was possible to verify a small reduction in the emulsified layer, with microscopy images revealing only slight signs of droplet coalescence. Taking into account the preliminary character of these tests, the obtained results are quite promising, supporting the exploitation of the developed CLPs for Pickering emulsions production, which can be applied in areas such as cosmetics and healthcare products [42,43].

Considering the conducted emulsifying tests and the effect of the process variables on the studied responses, CLPs 8, corresponding to an initial lignin concentration of 50 g/L, an antisolvent pH of 8, a final ethanol concentration of 45 %, and an antisolvent addition rate of 14 mL/min), revealed the most promising conditions to produce Pickering stabilizers. Particles with intermediary particle size and water contact angle (225 nm and 28º, respectively), high colloidal stability (zeta potential of −41 mV), and a light brown color (advantageous for commercial applications) were obtained. Their high potential as Pickering stabilizers was corroborated by the emulsifying tests. When CLPs 8 were used to stabilize a 50:50 Miglyol 812:water system, a stable emulsified layer (EL = 71%) was formed, remaining for 30 days. Therefore, CLPs 8 were chosen to inspect the particle morphology by TEM (Fig. 6). The performed analysis revealed a homogeneous size distribution of spherical and compact particles, with sizes circa 200 nm, consistent with the obtained by laser diffraction (225 nm). Overall, the TEM images revealed the formation of spherical particles with uniform size, which is an important feature for high-performance applications, such as in Pickering stabilization [6], a topic that will be deeper explored in future work.

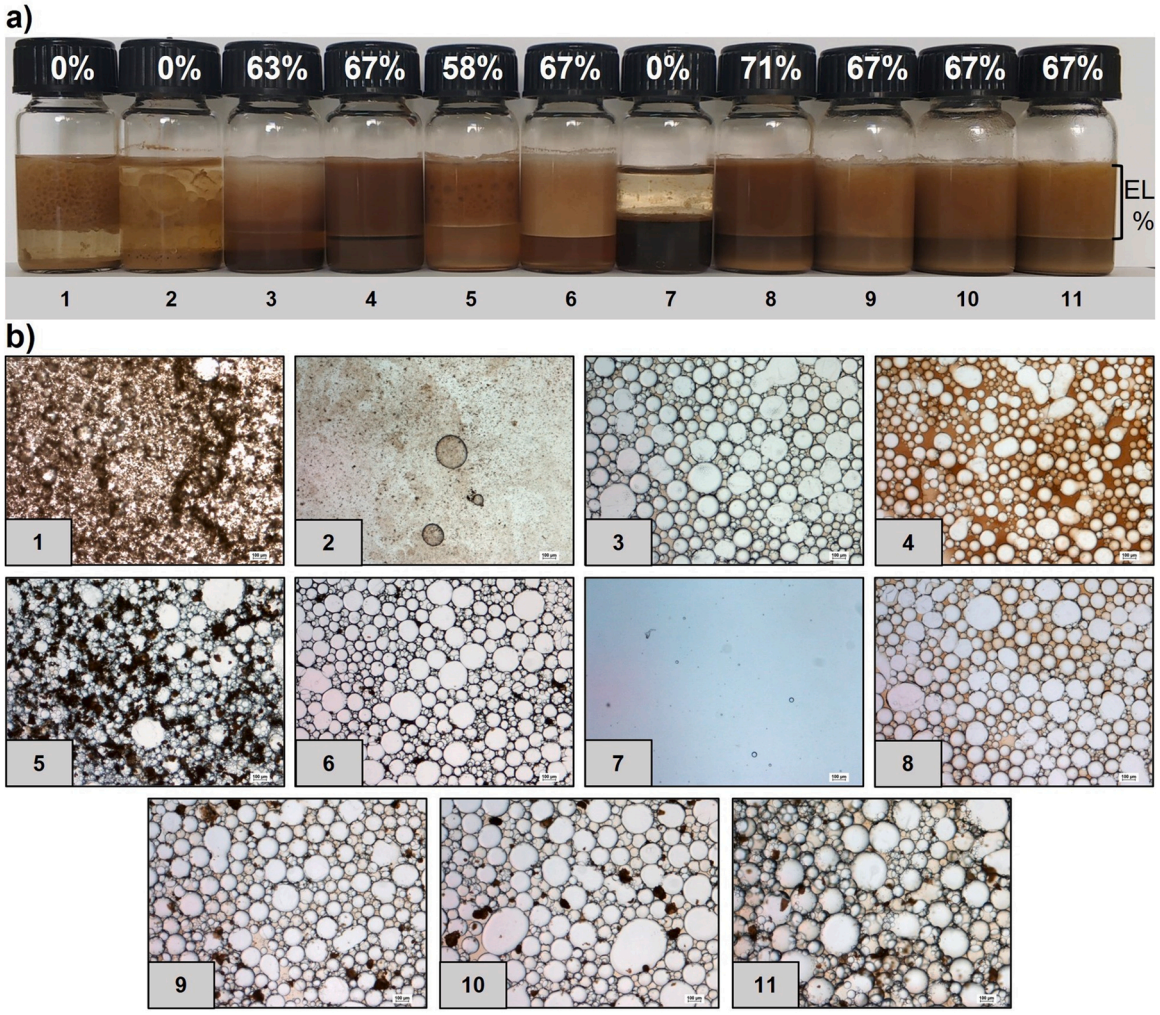

Fig. 5. (a) Images of the emulsions stored for 30 days at room temperature and percentage of the emulsified layer formed (EL%). (b) Optical microscopy of emulsions (emulsified layer). The bars in the bottom right corner indicate 100 μm - magnification of 40X.

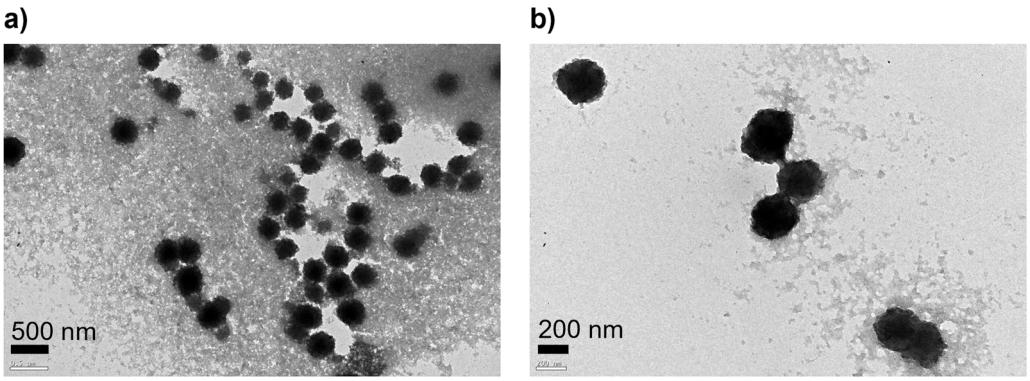

Fig. 6. TEM image of CLPs 8 under a magnification of a) 25,000× and b) 50,000×.

4. Conclusions

In this work, the individual effect of four process variables (initial lignin concentration, antisolvent pH, final ethanol concentration, and antisolvent rate addition) was studied to determine the most significant ones impacting CLPs properties, having in view their potential use as Pickering stabilizers. Through a screening design (FFD 2^{4-1}), 11 runs were performed, and the particle size, zeta potential, color, and contact angle were analyzed as responses. The most favorable conditions for preparing highly concentrated and stable CLPs with suitable characteristics to act as Pickering stabilizers corresponded to CLPs 8 (initial lignin concentration of 50 g/L, final ethanol concentration of 45%, antisolvent pH of 8, and antisolvent addition rate of 14 mL/min). The obtained CLPs presented intermediate size (circa 225 nm) and contact angle (circa 30º), high stability (zeta potential of −41 mV), a light brown color, and a high Pickering stabilizing potential. Overall, the screening design allowed the identification of the significant antisolvent precipitation variables and to perceive their individual effects on CLPs properties, which constituted valuable indicators to support the design of Pickering stabilizers. Thus, the next steps in this ongoing work will consider the optimization of Pickering emulsion production using tailored CLPs, targeting stability and technological properties of interest. Overall, this work can contribute to the development of new lignin-based solutions with the potential to be applied in different industrial sectors, such as cosmetics, pharmaceuticals, and food.

CRediT authorship contribution statement

Giovana Colucci: Conceptualization, Methodology, Investigation, Formal Analysis, Writing - Original Draft. **Arantzazu Santamaria-Echart:** Supervision, Writing - Review and Editing. **Samara C. Silva:** Investigation, Formal Analysis. **Liandra G. Teixeira:** Investigation. **Andreia Ribeiro:** Methodology, Investigation. **Alírio E. Rodrigues:** Supervision, Project Administration, Writing - Review and Editing. **M. Filomena Barreiro:** Conceptualization, Supervision, Resources, Project Administration, Funding Acquisition, Writing - Review and Editing.

Declaration of Competing Interest

The authors declare that they have no known competing financial interests or personal relationships that could have appeared to influence the work reported in this paper.

Data availability

Data will be made available on request.

Acknowledgments

The authors are grateful to the Foundation for Science and Technology (FCT, Portugal) for financial support through national funds FCT/MCTES (PIDDAC) to CIMO (UIDB/00690/2020 and UIDP/00690/2020), SusTEC (LA/P/0007/2021), LSRE-LCM (UIDB/50020/2020 and UIDP/00690/2020), and ALiCE (LA/P/0045/2020). National funding by FCT, P.I., through the institutional scientific employment program contract of A. Santamaria-Echart. FCT for the Ph.D. research grants of G. Colucci (2021.05215. BD), S.C. Silva (SFRH/BD/148281/2019), and L. G. Teixeira (2020.08803. BD). ValorNatural for A. Ribeiro contract (Norte01–0247-FEDER-024479). i3S Scientific Platform HEMS, member of the national infrastructure PPBI - Portuguese Platform of Bioimaging (PPBI-POCI-01–0145-FEDER-022122). Ingevity™ for the kind supply of Indulin AT lignin. COST Action LignoCOST (CA17128), supported by COST (European Cooperation in Science and Technology), in promoting interaction, exchange of knowledge, and collaborations in the field of lignin valorization.

Appendix A. Supporting information

Supplementary data associated with this article can be found in the online version at doi:10.1016/j.colsurfa.2023.131287.

References

[1] S. Cailotto, M. Gigli, M. Bonini, F. Rigoni, C. Crestini, Sustainable strategies in the synthesis of lignin nanoparticles for the release of active compounds: a comparison, ChemSusChem 13 (2020) 4759–4767, https://doi.org/10.1002/cssc.202001140.
[2] M.H. Sipponen, H. Lange, M. Ago, C. Crestini, Understanding lignin aggregation processes. A case study: budesonide entrapment and stimuli controlled release from lignin nanoparticles, ACS Sustain. Chem. Eng. 6 (2018) 9342–9351, https://doi.org/10.1021/acssuschemeng.8b01652.
[3] C.H.M. Camargos, C.A. Rezende, Antisolvent versus ultrasonication: bottom-up and top-down approaches to produce lignin nanoparticles (LNPs) with tailored properties, Int. J. Biol. Macromol. 193 (2021) 647–660, https://doi.org/10.1016/j.ijbiomac.2021.10.094.
[4] D. Piccinino, E. Capecchi, I. Delfino, M. Crucianelli, N. Conte, D. Avitabile, R. Saladino, Green and scalable preparation of colloidal suspension of lignin nanoparticles and its application in eco-friendly sunscreen formulations, ACS Omega 6 (2021) 21444–21456, https://doi.org/10.1021/acsomega.1c02268.
[5] W.D.H. Schneider, A.J.P. Dillon, M. Camassola, Lignin nanoparticles enter the scene: a promising versatile green tool for multiple applications, Biotechnol. Adv. 47 (2021), 107685, https://doi.org/10.1016/j.biotechadv.2020.107685.
[6] M. Österberg, M.H. Sipponen, B.D. Mattos, O.J. Rojas, Spherical lignin particles: a review on their sustainability and applications, Green Chem. 22 (2020) 2712–2733, https://doi.org/10.1039/D0GC00096E.
[7] C. Frangville, M. Rutkevičius, A.P. Richter, O.D. Velev, S.D. Stoyanov, V.N. Paunov, Fabrication of environmentally biodegradable lignin nanoparticles, ChemPhysChem 13 (2012) 4235–4243, https://doi.org/10.1002/cphc.201200537.
[8] F.M.C. Freitas, M.A. Cerqueira, C. Gonçalves, S. Azinheiro, A. Garrido-Maestu, A. A. Vicente, L.M. Pastrana, J.A. Teixeira, M. Michelin, Green synthesis of lignin nano- and micro-particles: physicochemical characterization, bioactive properties and cytotoxicity assessment, Int. J. Biol. Macromol. 163 (2020) 1798–1809, https://doi.org/10.1016/j.ijbiomac.2020.09.110.

[9] D.S. Bajwa, G. Pourhashem, A.H. Ullah, S.G. Bajwa, A concise review of current lignin production, applications, products and their environmental impact, Ind. Crops Prod. 139 (2019), 111526, https://doi.org/10.1016/j.indcrop.2019.111526.
[10] M.Y. Balakshin, E.A. Capanema, I. Sulaeva, P. Schlee, Z. Huang, M. Feng, M. Borghei, O.J. Rojas, A. Potthast, T. Rosenau, New opportunities in the valorization of technical lignins, ChemSusChem 14 (2021) 1016–1036, https://doi.org/10.1002/cssc.202002553.
[11] M. Ago, S. Huan, M. Borghei, J. Raula, E.I. Kauppinen, O.J. Rojas, High-throughput synthesis of lignin particles (~30 nm to ~2 μm) via aerosol flow reactor: size fractionation and utilization in pickering emulsions, ACS Appl. Mater. Interfaces 8 (2016) 23302–23310, https://doi.org/10.1021/acsami.6b07900.
[12] O. Gordobil, H. Li, A.A. Izquierdo, A. Egizabal, O. Sevastyanova, A. Sandak, Surface chemistry and bioactivity of colloidal particles from industrial kraft lignins, Int. J. Biol. Macromol. 220 (2022) 1444–1453, https://doi.org/10.1016/j.ijbiomac.2022.09.111.
[13] M.R.V. Bertolo, L.B. Brenelli de Paiva, V.M. Nascimento, C.A. Gandin, M.O. Neto, C.E. Driemeier, S.C. Rabelo, Lignins from sugarcane bagasse: renewable source of nanoparticles as Pickering emulsions stabilizers for bioactive compounds encapsulation, Ind. Crops Prod. 140 (2019), https://doi.org/10.1016/j.indcrop.2019.111591.
[14] H. Cuthill, C. Elleman, T. Curwen, B. Wolf, Colloidal particles for Pickering emulsion stabilization prepared via antisolvent precipitation of lignin-rich cocoa shell extract, Foods 10 (2021) 371, https://doi.org/10.3390/foods10020371.
[15] P.S. Chauhan, Lignin nanoparticles: eco-friendly and versatile tool for new era, Bioresour. Technol. Rep. 9 (2020), 100374, https://doi.org/10.1016/j.biteb.2019.100374.
[16] X. Liu, M. Xie, Y. Hu, S. Li, S. Nie, A. Zhang, H. Wu, C. Li, Z. Xiao, C. Hu, Facile preparation of lignin nanoparticles from waste Camellia oleifera shell: the solvent effect on the structural characteristic of lignin nanoparticles, Ind. Crops Prod. 183 (2022), https://doi.org/10.1016/j.indcrop.2022.114943.
[17] K.A. Henn, N. Forsman, T. Zou, M. Österberg, Colloidal lignin particles and epoxies for bio-based, durable, and multiresistant nanostructured coatings, ACS Appl. Mater. Interfaces 13 (2021) 34793–34806, https://doi.org/10.1021/acsami.1c06087.
[18] X. Wang, H. Guo, Z. Lu, X. Liu, X. Luo, S. Li, S. Liu, J. Li, Y. Wu, Z. Chen, Lignin nanoparticles: promising sustainable building blocks of photoluminescent and haze films for improving efficiency of solar cells, ACS Appl. Mater. Interfaces 13 (2021) 33536–33545, https://doi.org/10.1021/acsami.1c08209.
[19] L. Dai, Y. Li, F. Kong, K. Liu, C. Si, Y. Ni, Lignin-based nanoparticles stabilized pickering emulsion for stability improvement and thermal-controlled release of trans-resveratrol, ACS Sustain. Chem. Eng. 7 (2019) 13497–13504, https://doi.org/10.1021/acssuschemeng.9b02966.
[20] Y. Yang, J. Xu, J. Zhou, X. Wang, Preparation, characterization and formation mechanism of size-controlled lignin nanoparticles, Int. J. Biol. Macromol. 217 (2022) 312–320, https://doi.org/10.1016/j.ijbiomac.2022.07.046.
[21] J. Zhao, D. Zheng, Y. Tao, Y. Li, L. Wang, J. Liu, J. He, J. Lei, Self-assembled pH-responsive polymeric nanoparticles based on lignin-histidine conjugate with small particle size for efficient delivery of anti-tumor drugs, Biochem. Eng. J. 156 (2020), 107526, https://doi.org/10.1016/j.bej.2020.107526.
[22] Q. Cao, Q. Wu, L. Dai, C. Li, Y. Zhong, F. Yu, R. Li, C. Si, Size-controlled lignin nanoparticles for tuning the mechanical properties of poly(vinyl alcohol), Ind. Crops Prod. 172 (2021), 114012, https://doi.org/10.1016/j.indcrop.2021.114012.
[23] J. Adamcyk, S. Beisl, S. Amini, T. Jung, F. Zikeli, J. Labidi, A. Friedl, Production and properties of lignin nanoparticles from ethanol organosolv liquors-influence of origin and pretreatment conditions, Polymers 13 (2021) 1–13, https://doi.org/10.3390/polym13030384.
[24] M. Lievonen, J.J. Valle-Delgado, M.L. Mattinen, E.L. Hult, K. Lintinen, M. A. Kostiainen, A. Paananen, G.R. Szilvay, H. Setälä, M. Österberg, A simple process for lignin nanoparticle preparation, Green Chem. 18 (2016) 1416–1422, https://doi.org/10.1039/c5gc01436k.
[25] T. Leskinen, M. Smyth, Y. Xiao, K. Lintinen, M. Mattinen, M.A. Kostiainen, P. Oinas, M. Österberg, Scaling up production of colloidal lignin particles - OPEN ACCESS, Nord. Pulp Pap. Res. J. 32 (2017) 586–596, https://doi.org/10.3183/NPPRJ-2017-32-04-p586-596.
[26] Q. Xing, P. Buono, D. Ruch, P. Dubois, L. Wu, W.J. Wang, Biodegradable UV-blocking films through core-shell lignin-melanin nanoparticles in poly(butylene adipate- co-terephthalate), ACS Sustain. Chem. Eng. 7 (2019) 4147–4157, https://doi.org/10.1021/acssuschemeng.8b05755.
[27] X. Zhang, M. Yang, Q. Yuan, G. Cheng, Controlled preparation of corncob lignin nanoparticles and their size-dependent antioxidant properties: toward high value utilization of lignin, ACS Sustain. Chem. Eng. 7 (2019) 17166–17174, https://doi.org/10.1021/acssuschemeng.9b03535.
[28] M.I. Rodrigues, A.F. Iemma, Experimental Design and Process Optimization, CRC Press, 2014, https://doi.org/10.1201/b17848.
[29] S. Beisl, P. Loidolt, A. Miltner, M. Harasek, A. Friedl, Production of micro- and nanoscale lignin from wheat straw using different precipitation setups, Molecules 23 (2018), https://doi.org/10.3390/molecules23030633.
[30] W. Li, B. Jiao, S. Li, S. Faisal, A. Shi, W. Fu, Y. Chen, Q. Wang, Recent advances on pickering emulsions stabilized by diverse edible particles: stability mechanism and applications, Front. Nutr. 9 (2022) 1–17, https://doi.org/10.3389/fnut.2022.864943.
[31] L.E. Low, S.P. Siva, Y.K. Ho, E.S. Chan, B.T. Tey, Recent advances of characterization techniques for the formation, physical properties and stability of Pickering emulsion, Adv. Colloid Interface Sci. 277 (2020) 1–23, https://doi.org/10.1016/j.cis.2020.102117.
[32] C. Carriço, P. Pinto, A. Graça, L.M. Gonçalves, H.M. Ribeiro, J. Marto, Design and characterization of a new quercus suber-based pickering emulsion for topical application, Pharmaceutics 11 (2019) 1–16, https://doi.org/10.3390/pharmaceutics11030131.
[33] F. Xiong, Y. Han, S. Wang, G. Li, T. Qin, Y. Chen, F. Chu, Preparation and formation mechanism of size-controlled lignin nanospheres by self-assembly, Ind. Crops Prod. 100 (2017) 146–152, https://doi.org/10.1016/j.indcrop.2017.02.025.
[34] X. Li, J. Shen, B. Wang, X. Feng, Z. Mao, X. Sui, Acetone/water cosolvent approach to lignin nanoparticles with controllable size and their applications for pickering emulsions, ACS Sustain. Chem. Eng. 9 (2021) 5470–5480, https://doi.org/10.1021/acssuschemeng.1c01021.
[35] A.P. Richter, B. Bharti, H.B. Armstrong, J.S. Brown, D. Plemmons, V.N. Paunov, S. D. Stoyanov, O.D. Velev, Synthesis and characterization of biodegradable lignin nanoparticles with tunable surface properties, Langmuir 32 (2016) 6468–6477, https://doi.org/10.1021/acs.langmuir.6b01088.
[36] A. Manisekaran, P. Grysan, B. Duez, D.F. Schmidt, D. Lenoble, J.-S. Thomann, Solvents drive self-assembly mechanisms and inherent properties of Kraft lignin nanoparticles (<50 nm), J. Colloid Interface Sci. 626 (2022) 178–192, https://doi.org/10.1016/j.jcis.2022.06.089.
[37] P.K. Mishra, A. Ekielski, The self-assembly of lignin and its application in nanoparticle synthesis: a short review, Nanomaterials 9 (2019) 1–15, https://doi.org/10.3390/nano9020243.
[38] J. Laine, L. Lövgren, P. Stenius, S. Sjöberg, Potentiometric titration of unbleached kraft cellulose fibre surfaces, Colloids Surf. A Physicochem. Eng. Asp. 88 (1994) 277–287, https://doi.org/10.1016/0927-7757(94)02834-6.
[39] W. Zhang, J. Shen, P. Gao, Q. Jiang, W. Xia, An eco-friendly strategy for preparing lignin nanoparticles by self-assembly: characterization, stability, bioactivity, and pickering emulsion, Ind. Crops Prod. 188 (2022), 115651, https://doi.org/10.1016/j.indcrop.2022.115651.
[40] S.C. Lee, E. Yoo, S.H. Lee, K. Won, Preparation and application of light-colored lignin nanoparticles for broad-spectrum sunscreens, Polymers 12 (2020) 699, https://doi.org/10.3390/polym12030699.
[41] B.P. Binks, Particles as surfactants—similarities and differences, Curr. Opin. Colloid Interface Sci. 7 (2002) 21–41, https://doi.org/10.1016/S1359-0294(02)00008-0.
[42] O. Gordobil, P. Olaizola, J.M. Banales, J. Labidi, Lignins from agroindustrial by-products as natural ingredients for cosmetics: chemical structure and in vitro sunscreen and cytotoxic activities, Molecules 25 (2020) 1–16, https://doi.org/10.3390/molecules25051131.
[43] N. Sajinčič, O. Gordobil, A. Simmons, A. Sandak, An exploratory study of consumers' knowledge and attitudes about lignin-based sunscreens and bio-based skincare products, Cosmetics 8 (2021) 78, https://doi.org/10.3390/cosmetics8030078.